SUPPLEMENTARY INFORMATION TO

Copper and its isotopes in organic-rich sediments: from the modern Peru Margin to Archean shales

S1. Peru Margin sample location and details

The Peru margin, along with the Chilean margin, is considered as the most productive up- welling system in the world ocean [S1], driven mainly by the southeast trade winds [S2]. The hydrography is dominated by the Peru Current, with the poleward Peruvian Undercurrent and the equatorward Chile-Peru Deep Coastal Current being the main coastal currents [S3-S4, and references therein]. The upwelling-fed high productivity of this region results in the permanent eastern South Pacific oxygen minimum zone (OMZ), with its core located between 5 and 13°S. At these latitudes the OMZ reaches its maximal vertical thickness of about 600 m, with an upper boundary at ≤ 100 m water depth [S1]. The vertical thickness of the OMZ and the location of its upper boundary, however, fluctuate with the El Niño Southern Oscillation (ENSO) cycle, as well as with the variable influence of the southeast trade winds and northerly winds off the coasts of Peru and Chile [S1]. The seafloor below the OMZ and along the margin is dominated by two main sedimentary facies: (i) a lens-shaped, up to 100m thick, diatomaceous (up to ~16wt.% opal), organic-rich mud at depths between 50 and 500m at 11-14°S; and (ii) a coarser-grained, less organic-rich, calcareous mud on the shallow shelf at 8.5°S and 15-17°S [S5]. Thus, the most organic-rich sediments are deposited between 11 and 14° S, which are the latitudes targeted here.

Peru Margin sediment cores were recovered as box cores and multicores in October-November 1992 during a cruise of R/V Seward Johnson, and as multicores in October-November 2005 during cruise 182-9 of R/V Knorr. Upon recovery, all cores were immediately sliced at 0.5 – 1.0 cm intervals, stored in glass jars or plastic sampling bags, and frozen. In this study we focused on core-tops recovered by R/V Seward Johnson and multiple down-core samples from three of the cores recovered by R/V Knorr (Fig. S1; Table S1), in order to cover a range of redox conditions and organic matter contents. Prior to processing, the samples were freeze dried and subsamples of ~1g were weighed into 60ml Teflon beakers for subsequent acid digestion.

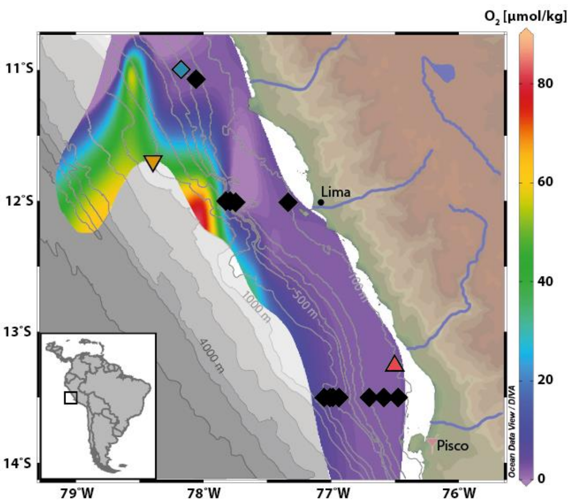

Figure S1. Details of the Peru Margin setting, where core-top samples (black diamonds) and three down-core profiles (colored symbols) were taken.

Table S1. Peru Margin sediment core locations

core ID	lat/long [°N/°E]	depth [m]	bottom O_2 [μM]	location wrt OMZ
R/V Seward Johnson 10-92				
BC39	-13.509 / -76.927	550	10	within OMZ
BC57	-13.512 / -76.695	172	<10	within OMZ
BC62	-13.499 / -76.959	643	10	below OMZ
BC76	-13.502 / -76.983	725	15	below OMZ
BC81	-13.508 / -76.578	130	10	within OMZ
KC83	-13.518 / -76.473	106	10	upper OMZ
BC93	-12.000 / -77.335	100	5	upper OMZ
BC125	-11.998 / -77.807	340	5	within OMZ
KC127	-11.996 / -77.790	309	5	within OMZ
BC153	-11.062 / -78.073	250	5	within OMZ
R/V Knorr 182-9				
MC6A	-13.250 / -76.500	100	2	upper OMZ
MC9G	-11.718 / -78.399	1500	80	below OMZ
MC11C	-11.000 / -78.167	325	2	within OMZ

S2. Geological record sample details

The geological record sample set consists of 50 samples from 27 formations, ranging in age from Archean to Ordovician/Silurian. These are all organic-rich shales, sampled from lithologies that underwent, at most, lower greenschist facies metamorphism. A brief overview of location, lithologies, metamorphic grade, and age constraints is provided below for each subset of samples, organised by geological formations. These samples were provided by Prof.Simon Poulton (University of Leeds), Prof. Axel Hofmann (University of Johannesburg), and Dr. Xi Chen (Nanjing University), as either powders or quarter-cores from drill core or hand samples collected in the field.

~ 0.45 Ga Wufeng and Longmaxi formations, Guizhou Basin, China

A total of six black shale samples from the Wufeng and Longmaxi Formations of the Guizhou basin in China, were selected for this study. The Wufeng-Longmaxi Fm. shales are currently one of the main sources of shale gas in the Sichuan basin [S6-S7], and most studies on these lithologies have focused on the source and reservoir characteristics of these formations. The Wufeng-Longmaxi shales were deposited during the Late Ordovician and Early Silurian, in restricted basins that formed upon compression of the Sichuan basin in the Late Ordovician that gave rise to the orogenic belts surrounding the Sichuan and Guizhou basins Ye et al. [S8].

~ 0.53-0.50 Ga Georgina Basin, Australia

The Georgina basin formed by disruption of the Centralian Superbasin by the Peterman Orogeny (570 - 530 Ma; [S9]) and the Alice Springs Orogeny (450 - 300 Ma; [S10]). We analyzed Cambrian black shales from three formations sampled from drillcore Baldwin-1, which was drilled in the southern Georgina basin [S11]. The Red Heart Dolostone Fm. is described as a carbonate succession mostly known for its archaeocyath-bearing dolostone [S11] and is part of the Shadow Group, deposited during the Terreneuvian (or possibly during Series 2 Stage 3 of the Cambrian; [S12]). The Red Heart Fm. is unconformably overlain by the sediments of the Narpa Group, which is made up of the Thorntonia Limestone, Arthur Creek Fm., Steamboat Sandstone, and Arrinthrunga Fm. Based on trilobite biozones, deposition of the Thorntonia Limestone is correlative with Series 2 Stage 4 (or possibly Series 3 Stage 5 [S12]), while deposition of the overlying anoxic sediments of the Arthur Creek Fm. is correlative with Series 2 Stage 4 up to the Guzhangian of Series 3 [S12]. The

~ 510 Ma Kalkarindji Flood Basalt lies stratigraphically between the Thorntonia Limestone and Arthur Creek Fm [S13-S14]. Based on this age, and the above chronostratigraphic correlation, ages of 521 Ma, 515 Ma, and 505 Ma were assigned to samples from the Red Heart Dolostone, Thorntonia Limestone, and Arthur Creek Fm., respectively.

~ 0.52-0.57 Ga Officer Basin, Australia

The Officer basin is another of the many basins that formed upon disruption of the Centralian Superbasin by the Petermann and Alice Springs Orogenies. The Colmaco exploration well Munta-1 was drilled in the eastern part of the Officer basin and includes the Cambrian-Ediacaran lithologies of the Ungoolya Group. Shale samples used in this study are from four formations that make up most of the Ungoolya Group and are, in stratigraphic order from oldest to youngest, the Tanana, Munyarai, Narana, and Observatory Hill formations, which are dominantly composed of laminated mudstone and carbonates. Due to the lack of geochronological data, age constraints on the lithologies within the Officer basin are mostly based upon interbasinal correlations of units across the Centralian Superbasin, isotope stratigraphy, and chronologically diagnostic fossil assemblages such as acritarch biostratigraphy. Taking from this, Wade et al. [S15] assign ages of 520 Ma, 560 Ma, and 570 Ma to the Observatory Hill Fm, the Mena Mudstone Member, and the Tanana Fm., respectively. Given that the Munyarai Fm. and Narana Fm. lie between the Tanana Fm. and the Mena Mudstone Member, we assign an indicative age of 565 Ma to both.

~ 0.83 Ga Finke beds, Amadeus Basin, Australia

We studied one sample from drill-core Wallara-1, at 1486.3 cm depth in the core, which is described by Gorjan et al. [S16] and Guilbaud et al. [S17] as belonging to the Finke beds. The Finke beds have recently been renamed as the Wallara Formation. As there is limited outcrop exposure in the Amadeus Basin, this formation is best described from drillcore Wallara-1 as dolostone interbedded with dolomitic siltstones and shales occasionally containing pyrite and glauconite [S18]. According to Schmid et al. [S18] the Wallara Fm. is included in the Bitter Springs Package, which comprises the Gillen, Loves Creek, Johnny's Creek, and finally the Wallara Formations. Walter et al. [S19] date the boundary between the Gillen Member and the Loves Creek member at 834 Ma (Rb-Sr dating). Based on correlations of carbon isotope data from the Bitter Springs Group with that of the Fifteen Mile Group on NW Canada and of the Ombobo Supergroup of Namibia, Swanson-Hysell et al. [S20] constrain the deposition of the Love's Creek Member at 810 - 785 Ma and of the top of the Johnny's Creek Member to ~ 750 Ma. Hence, with these being the constraints available we assign an age of ~ 750 Ma to the Wallara sample studied here, though this is most likely an upper estimate and it could be younger.

~ 1.10 Ga Tourist and Aguelt el Mabha formations, Taudeni Basin, Mauritania

We studied samples from two formations in the Atar/El Mreiti Group, the Tourist Fm. and the Aguelt el Mabha Fm. of the Taoudeni Basin, which is thought to have been unaffected by any significant post-depositional metamorphism [S21]. The age constraint of ~ 1100 Ma comes from Re-Os geochronology [S21]. Dates previously obtained by Rb-Sr illite and glauconite geochronology are ~ 200 Ma younger, but these are now thought to record diagenetic events and not the primary deposition age. Samples are from two drill cores, S2 and S3 described in Rooney et al. [S21]. All samples are dark grey or black shales. Iron speciation analyses on samples from three Total S.A. cores (including S2) suggest that the Tourist Fm. shales were deposited in an anoxic ferruginous setting with possible occasional euxinia [S22]. On the other hand, fluctuations between oxic and euxinic depositional settings were invoked by Gilleaudeau and Kah [S23] for Tourist Fm shales sampled from different cores. Therefore, a certain degree of heterogeneity is inferred in terms of depositional setting within the samples of this formation. Iron speciation analyses on Aguelt el Mabha Fm samples suggest deposition in oxic and ferruginous conditions, with some samples giving equivocal results [S23-S22]. Unfortunately, iron speciation data for the specific samples analyzed in this study are not yet available.

~ 1.40 Ga Velkerri Formation, McArthur Basin, Australia
The Velkerri Formation is part of the Roper Group, deposited in the McArthur Basin of northern Australia. The dominant lithologies are un-metamorphosed mudstone and shale deposited in a low-energy, outer-shelf environment [S24-S25]. Re-Os geochronology on the upper and lower Velkerri Fm. provides ages of 1361 ± 21 Ma and 1417 ± 29 Ma, respectively [S26]. For this study we sampled two shales from drill-core BMR Urapunga-4 [S25]. Although the exact samples studied here were not processed for iron speciation analyses, samples at depths bracketing them are all interpreted as being deposited in euxinic settings [S27].

~ 1.64 Ga Barney Creek, McArthur Basin, Australia
The Barney Creek Formation was deposited in the Batten Fault Zone within the McArthur Basin of Northern Australia and is dated at 1639 ± 2 Ma by U-Pb SHRIMP geochronology of tuff layers within the formation [S28]. The Barney Creek Fm. has been at the center of previous studies as it hosts the HYC deposit, one of the largest Proterozoic sediment-hosted Pb/Zn/Ag deposits [S29]. It has also been studied for its extremely well-preserved organic matter and the organic biomarkers extracted from it [e.g., S30-S32]. The lithology consists mainly of laminated carbonaceous, dolomitic, and pyritic siltstones and shales [S31], which are interpreted as a marine succession [S27,S33-S34] though previously thought to be of lacustrine, sabkha origin [S35]. Here we analyzed three carbonaceous shales and one pyritic black shale sample from drill core GRNT 79-7 (or GR-7) of the Glyde River sub-basin (see Lee and Brocks, [S32], for core lithologies).

~ 1.84 Ga Rove and Virginia formations, Animike Basin, North America
The Animikie Basin is located in the south-western margin of the Superior Province of North America and contains sediments deposited in an open-ocean setting. Here we analyzed shale samples from two formations, the Rove Fm. (core PR98-1), present in the northern portion of the basin, and the Virginia Fm. (core MGS2), located in the southern part of the basin [S36]. The Rove and Virginia formations consist mainly of carbonaceous shales, siltstones and sandstones [S36]. The two formations are separated by a Mesoproterozoic intrusion. The sediments in its proximity are affected by contact metamorphism whereas otherwise the rocks in the north are sub-greenschist facies and in the south of lower greenschist [S37]. Tuffaceous layers in the Rove and Virginia formations give U-Pb zircon ages of 1836 ± 5 Ma [S38]. Iron speciation indicates deposition from a strongly stratified ocean, ferruginous at depth, oxic at the surface, and euxinic at mid-depths [S36].

~ 2.02 Ga Wildman Siltstone, Mount Partridge Group, Pine Creek, Australia
The Wildman Siltstone is part of the Mount Partridge Group deposited in the Pine Creek succession of the North Australia Craton [S39]. SHRIMP U-Pb analyses of tuffaceous siltstone from the Wildman Siltstone provide an age of 2019 ± 4 Ma [S40]. The dominant lithologies in the formation are grey siltstone, carbonaceous shale and some dolostone [S39]. Two shale samples from drill core 77BLD3 of the Northern Territory Geological Survey were analysed here. Iron speciation characterization of these samples indicate they were deposited under ferruginous conditions (Poulton et al., pers. comm).

~ 2.32 Ga Timeball Hill Formation, Pretoria Group, South Africa
The Timeball Hill Formation belongs to the lower part of the Pretoria Group of the Transvaal Supergroup in South Africa. It mostly consists of lower greenschist facies shales and siltstones deposited in a shallow marine setting, with an upper and lower unit separated by a quartzite middle unit [S41]. Pyrite within carbonaceous shales at the boundary between the Timeball Hill Formation and the underlying Rooihoogte Formation is well constrained in age at 2316 ± 7 Ma by Re-Os geochronology [S42]. Three black shale samples from core EBA-1 were studied here and, based on global redox settings suggested by Rouxel et al. [S43] on the basis of Fe isotopes analysed on these and other samples of similar age, they were likely deposited under ferruginous conditions.

~2.4-2.6 Ga Hamersley Basin, Australia

The Hamersley Group deposited in the Hamersley Basin of western Australia, consists of the following formations, in depositional order from the youngest to the oldest: Boolgeeda Iron Formation, Woongarra Rhyolite, Weeli Wolli Formation, Brockman Iron Formation, Mt. McRae Shale, Wittenoom Formation, and Marra Mamba Iron Formation. In this study a total of four shales were analyzed from the Hamersley Group; two samples from the Whaleback Shale Member of the Brockman Iron Formation, one sample from the Mt. McRae Shale, and one sample from the Marra Mamba Iron Formation (MMIF). The two Whaleback Shale samples and the Mt. McRae Shale sample were provided by Prof. Simon Poulton (Leeds University) and, unfortunately, core information for these is not available. The MMIF shale sample was taken from core WRL-1. The highest degree of metamorphism experienced within the Hamersley Basin, and hence by these samples, was of sub-greenschist facies [S44]. An age of 2597 ± 5 Ma is assigned to the MMIF by SHRIMP U-Pb zircon geochronology of a sample from the Mt. Newman Formation [S45]. The age of the Mt.McRae Shale is constrained by the overlying crystal-rich tuff of the Wittenoom Formation, dated at 2561 ± 8 Ma [S45], and the underlying Dales Gorge Member, dated at 2479 ± 3 Ma. The Whaleback Shale Member has been dated at 2463 ± 5 Ma [S46].

~2.5-2.7 Ga Schmidtsdrift and Campbellrand/Malmani Sub-groups, Transvaal Su- pergroup, Kaapvaal Craton, South Africa

The Schmidtsdrift siliciclastic-carbonate succession and the Campbellrand/Malmani carbonate platform succession form sub-groups of the Transvaal Supergroup in the Kaapvaal Craton of South Africa. Except for local higher-grade metamorphism, these sediments only experienced sub-greenschist metamorphism [S47]. The Schmidtsdrift Sub-group consists, from its base, of the Vryburg Formation, Boomplas Formation, and the Lokammona Formation, which is overlain by the Monteville, Nauga, and Klein Naute formations of the Campbellrand/Malmani Sub-group [S48]. Despite the dominant carbonate lithology, several thick shale successions are also present within these formations. For the purpose of this study shales of the Vryburg, Upper Nauga, and Klein Naute formations were sampled from the Agouron core GKP-01, drilled to the south-east of Griquatown. SHRIMP U-Pb zircon geochronology from tuff beds within the Vryburg Formation indicate a depositional age of 2669 ± 5 Ma [S48]. An age of about 2521 Ma is assigned by Knoll and Beukes [S48] to the uppermost portion of the Upper Nauga Formation based on correlative relationships of tuff layers dated by whole zircon ID TIMS U-Pb (2521 ± 3 Ma; Sumner and Bowring, [S49]) and SHRIMP U-Pb geochronology (2516 ± 4 Ma; [S50]). The age of the Klein Naute Fm. is bracketed by that of the Upper Nauga and of the Riries Member of the Kuruman Iron Formation, dated at 2460 ± 5 Ma by SHRIMP U-Pb geochronology [S51]. Iron speciation analysis of samples from core GKP-01 suggest that the shales analyzed here from the Klein Naute and Upper Nauga formations were deposited in an intermittently euxinic setting [S52].

~ 2.95 Ga Mozaan Group, Pongola Supergroup, Kaapvaal Craton, South Africa

The Mozaan Group, together with the Nsuze Group, is part of the volcano-sedimentary Pongola Supergroup deposited on the Kaapvaal Craton of South Africa. The Mozaan Group consists of marine sandstones, shales, and banded iron formations (BIF), metamorphosed to lower greenschist facies grade [S53-S54]. The basal part of the Mozaan Group comprises the ~ 2.95 Ga Sinqeni Formation and the overlying Ntombe Formation, both containing sandstone, shale and siltstone [S55-S56]. This study includes analyses of six shales sampled from drill core TSB07-26. Previous studies on samples from this same core suggest that considerable enrichments in Mn and correlations between Fe/Mn ratios and molybdenum isotopes indicate possible deposition in an 'oxygen oasis' setting, where oxygen was available in surface shallow waters [S57-S58].

~ 3.3-3.4 Ga Onverwacht Group, Barberton Greenstone Belt, South Africa

The Barberton Greenstone Belt (BGB) is a volcano-sedimentary sequence located in South Africa at the border between Mpumalanga Province and Swaziland. The BGB is divided into three groups, the Onverwacht (3.5 - 3.3 Ga), Fig Tree (3.3 - 3.2 Ga), and Moodies (3.2 Ga) groups [S59]. The

Onverwacht Group consists mostly of mafic and ultramafic volcanics, with some thin layers of chert. The Fig Tree Group consists of shales, sandstones, volcanic deposits, chert, and BIF. The Moodies Group consists of sandstones, shales, conglomerates, and BIF. The metamorphic grade experienced by these rocks is of lower greenschist facies [S59-S60]. In this study samples from the two uppermost formations of the Onverwacht Group were analysed. Three samples are from the Buck Reef Chert, in the Kromberg Formation, and were sampled from the ICDP "Barberton Drilling Project" BARB3 core. One sample is from the overlying Mendon Formation and was sampled from core BARB4 of the same drilling project. A Pb-Pb age of 3416 ± 5 Ma was determined from the analyses of zircons from the base of the Buck Reef Chert [S61]. The upper part of the Mendon Formation yielded zircon ages of 3.28 Ga.

S3. Test of the two-step digestion methodology

A schematic representation of the approach undertaken to test the two-step digestion method is shown in Fig. S2 and the resulting concentrations and isotope compositions for each OPF and HFD fraction are reported in Table S2 and illustrated in Figure S3.

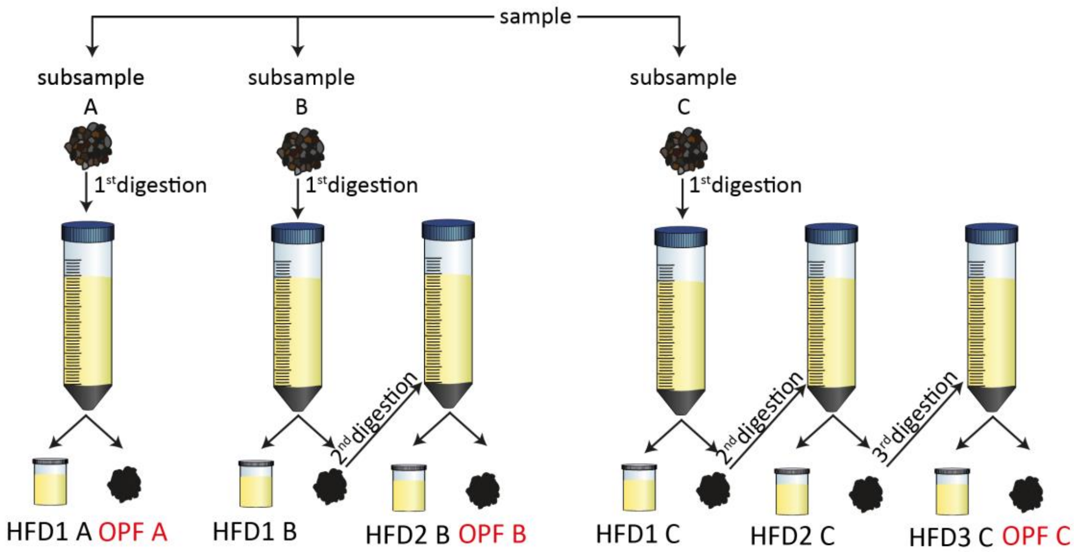

Figure S2. Schematic representation of the method validation experiment. All subsample digestions were repeated in complete duplicate but only one is shown here.

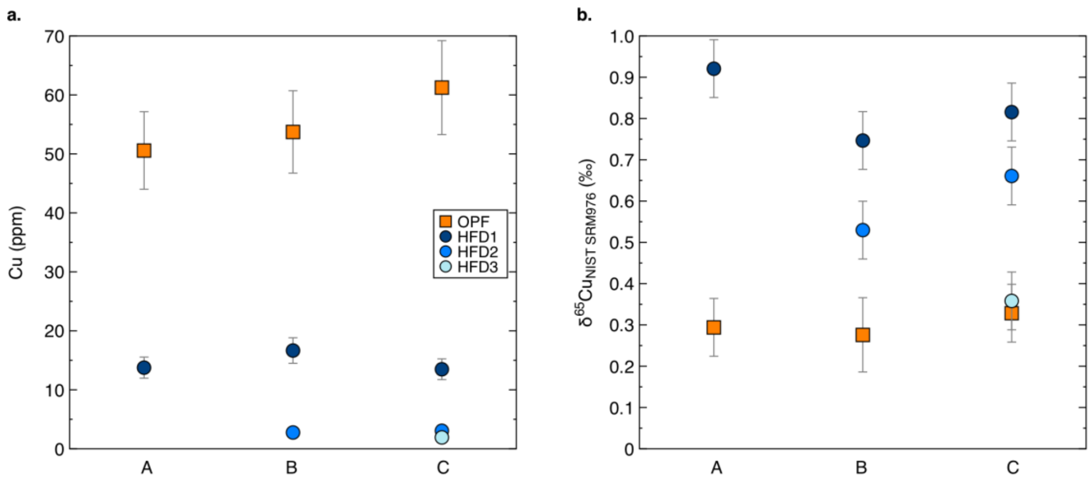

Figure S3. Cu concentrations (a) and isotope compositions (b) for each of the three method validation steps. Error bars indicate the long-term external reproducibility (2σ).

Table S2. Results of test on two-step digestion methodology

Sample		Duplicate 1			Duplicate 2			Average		
		Cu Elem[1] (ppm)	δ^{65}Cu (‰)	2σ	Cu Elem[1] (ppm)	δ^{65}Cu (‰)	2σ	Cu Elem[1] (ppm)	δ^{65}Cu (‰)	2σ[2]
BC81A	OPF	24	0.39	0.03	51	0.25	0.05	51	0.29	0.07
BC81A	HFD1	14	0.98	0.05	14	0.86	0.04	14	0.92	0.07
BC81B	OPF	54	0.30	0.04	53	0.25	0.15	54	0.28	0.09
BC81B	HFD1	17	0.73	0.04	17	0.76	0.03	17	0.75	0.07
BC81B	HFD2	3.5	0.52	0.04	2.0	0.54	0.03	2.8	0.53	0.07
BC81C	OPF	73	0.34	0.04	49	0.31	0.03	61	0.33	0.07
BC81C	HFD1	5.8	0.67	0.04	13	0.88	0.03	13	0.82	0.07
BC81C	HFD2	3.1	0.73	0.03	3.0	0.59	0.04	3.1	0.66	0.07
BC81C	HFD3	1.9	0.47	0.06	2.0	0.25	0.04	1.9	0.36	0.07

1Concentrations obtained via ElementXR analyses

2All duplicate analyses agree to a level that is consistent with the long-term reproducibility and this is used as the uncertainty here and in Fig. S3

References

S1. Fuenzalida, R.; Schneider, W.; Garcés-Vargas, J.; Bravo, L.; Lange, C. Vertical and horizontal extension of the oxygen minimum zone in the eastern South Pacific Ocean. *Deep Sea Research Part II: Topical Studies in Oceanography* **2009**, 56 (16), 992–1003. doi: 10.1016/j.dsr2.2008.11.001

S2. Smith, R. L. Circulation patterns in upwelling regimes. In: Coastal Upwelling: Its Sediment Record, Part A, Suess, E.; Thiede, J. (Eds.),Plenum, New York, **1983**, 13–35.

S3. Brockmann, C.; Fahrbach, E.; Huyer, A.; Smith, R. L. The poleward undercurrent along the Peru coast: 5° to 15°S. *Deep Sea Research Part A. Oceanographic Research Papers* **1980**, 27 (10), 847–856. doi: 10.1016/0198-0149(80)90048-5

S4. Erdem, Z.; Schönfeld, J.; Glock, N.; Dengler, M.; Mosch, T.; Sommer, S., Elger, J.; Eisenhauer, A. Peruvian sediments as recorders of an evolving hiatus for the last 22 thousand years. *Quaternary Science Reviews* **2016**, 137, 1–14. doi: 10.1016/j.quascirev.2016.01.029

S5. Suess, E.; Kulm, L. D.; Killingley, J. S. Coastal upwelling and a history of organic-rich mudstone deposition off Peru. *Geological Society, London, Special Publications* **1987**, 26 (1), 181–197. doi: 10.1144/GSL.SP.1987.026.01.11

S6. Yang, R.; He, S.; Wang, X.; Hu, Q.; Hu, D.; Yi, J. Paleo-ocean redox environments of the Upper Ordovician Wufeng and the first member in lower Silurian Longmaxi formations in the Jiaoshiba area, Sichuan Basin. *Can. J. Earth Sci.* **2016**, 53 (4), 426–440. doi: 10.1139/cjes-2015-0210

S7. Liang, C.; Jiang, Z.; Cao, Y.; Zhang, J.; Guo, L. Sedimentary characteristics and paleoenvi- ronment of shale in the Wufeng-Longmaxi Formation, North Guizhou Province, and its shale gas potential. *J. Earth Sci.* **2017**, 28 (6), 1020–1031. doi: 10.1007/s12583-016-0932-x

S8. Ye, Y.-H.; Liu, S.-G.; Ran, B.; Luba, J.; Wang, S.-Y.; Sun, W.; Yang, D.; Luo, C. Characteristics of black shale in the Upper Ordovician Wufeng and lower Silurian Longmaxi formations in the Sichuan Basin and its periphery, China. *Australian Journal of Earth Sciences* **2017**, 64 (5), 667–687. doi: 10.1080/08120099.2017.1321581

S9. Walter, M. R.; Veevers, J. J.; Calver, C. R.; Grey, K. Neoproterozoic stratigraphy of the Centralian Superbasin, Australia. *Precambrian Research* **1995**, 73 (1), 173–195. doi: 10.1016/0301-9268(94)00077-5

S10. Maidment, D. W.; Hand, M.; Williams, I. S. Tectonic cycles in the Strangways Metamorphic Complex, Arunta Inlier, central Australia: geochronological evidence for exhumation and basin formation between two high-grade metamorphic events. *Australian Journal of Earth Sciences* **2005**, 52 (2), 205–215. doi: 10.1080/08120090500139414

S11. Ambrose, G. J.; Kruse, P. D.; Putnam, P. E. Geology and hydrocarbon potential of the southern Georgina Basin, Australia. *The APPEA Journal* **2001**, 41 (1), 139–163. doi: 10.1071/aj00007
S12. Creveling, J. R.; Johnston, D. T.; Poulton, S. W.; Kotrc, B.; Marz, C.; Schrag, D. P.; Knoll, A. H. Phosphorus sources for phosphatic Cambrian carbonates. *Geological Society of America Bulletin* **2013**, 126 (1-2), 145-163. doi: 10.1130/B30819.1
S13. Hough, M. L.; Shields, G. A.; Evins, L. Z.; Strauss, H.; Henderson, R. A.; Mackenzie, S. A major sulphur isotope event at c. 510 Ma: a possible anoxia–extinction–volcanism connection during the Early–Middle Cambrian transition? *Terra Nova* **2006**, 18 (4), 257–263. doi: 10.1111/j.1365-3121.2006.00687.x
S14. Pagès, A.; Schmid, S.; Edwards, D.; Barnes, S.; He, N.; Grice, K. A molecular and isotopic study of palaeoenvironmental conditions through the middle Cambrian in the Georgina Basin, central Australia. *Earth and Planetary Science Letters* **2016**, 447, 21–32. doi: 10.1016/j.epsl.2016.04.032
S15. Wade, B. P.; Hand, M.; Barovich, K. M. Nd isotopic and geochemical constraints on provenance of sedimentary rocks in the eastern Officer Basin, Australia: implications for the duration of the intracratonic Petermann Orogeny. *Journal of the Geological Society* **2005**, 162 (3), 513–530. doi: 10.1144/0016-764904-001
S16. Gorjan, P.; Veevers, J. J.; Walter, M. R. Neoproterozoic sulfur-isotope variation in Australia and global implications. *Precambrian Research* **2000**, 100 (1), 151–179. doi: 10.1016/S0301-9268(99)00073-X
S17. Guilbaud, R.; Poulton, S. W.; Butterfield, N. J.; Zhu, M.; Shields-Zhou, G. A. A global transition to ferruginous conditions in the early Neoproterozoic oceans. *Nature Geoscience* **2015**, 8 (6), 466–470. doi: 10.1038/ngeo2434
S18. Schmid, S.; Kunzmann, M.; Pagès, A. Inorganic geochemical evaluation of hydrocarbon source rock potential of Neoproterozoic strata in the Amadeus Basin, Australia. *Marine and Petroleum Geology* **2017**, 86, 1092–1105. doi: 10.1016/j.marpetgeo.2017.07.015
S19. Walter, M. R.; Veevers, J. J.,;Calver, C. R.; Gorjan, P.; Hill, A. C. Dating the 840–544 Ma Neoproterozoic interval by isotopes of strontium, carbon, and sulfur in seawater, and some interpretative models. *Precambrian Research* **2000**, 100 (1), 371–433. doi: 10.1016/S0301-9268(99)00082-0
S20. Swanson-Hysell, N. L.; Maloof, A. C.; Kirschvink, J. L.; Evans, D. A. D.; Halverson, G. P.; Hurtgen, M. T. Constraints on Neoproterozoic paleogeography and Paleozoic orogenesis from pale- omagnetic records of the Bitter Springs Formation, Amadeus Basin, central Australia. *American Journal of Science* **2012**, 312 (8), 817–884. doi: 10.2475/08.2012.01
S21. Rooney, A. D;, Selby, D.; Houzay, J.-P.; Renne, P. R. Re–Os geochronology of a Mesoproterozoic sedimentary succession, Taoudeni basin, Mauritania: Implications for basin-wide correlations and Re–Os organic-rich sediments systematics. *Earth and Planetary Science Letters* **2010**, 289 (3), 486–496. doi: 10.1016/j.epsl.2009.11.039
S22. Beghin, J.; Guilbaud, R.; Poulton, S. W.; Gueneli, N.; Brocks, J. J.; Storme, J.-Y.; Blanpied, C.; Javaux, E. J. A palaeoecological model for the late Mesoproterozoic – early Neoproterozoic Atar/El Mreïti Group, Taoudeni Basin, Mauritania, northwestern Africa. *Precambrian Research* **2017**, 299, 1–14. doi: 10.1016/j.precamres.2017.07.016
S23. Gilleaudeau, G. J.; Kah, L. C. Heterogeneous redox conditions and a shallow chemocline in the Mesoproterozoic ocean: Evidence from carbon–sulfur–iron relationships. *Precambrian Research* **2015**, 257, 94–108. doi: 10.1016/j.precamres.2014.11.030
S24. Sweet, I. P.; Jackson, M. J. BMR stratigraphic drilling in the Roper Group, Northern Territory, 1985. *Bureau Mineral Resources Geology and Geophysics Australia Record* **1986**, (19).
S25. Jackson, M. J.; Raiswell, R. Sedimentology and carbon-sulphur geochemistry of the Velkerri Formation, a mid-Proterozoic potential oil source in northern Australia. *Precambrian Research* **1991**, 54 (1), 81–108. doi: 10.1016/0301-9268(91)90070-Q
S26. Kendall, B.; Creaser, R. A.; Gordon, G. W.; Anbar, A. D. Re–Os and Mo isotope systematics of black shales from the Middle Proterozoic Velkerri and Wollogorang Formations, McArthur Basin, northern Australia. *Geochimica et Cosmochimica Acta* **2009**, 73 (9), 2534–2558. doi: 10.1016/j.gca.2009.02.013
S27. Shen, Y.; Knoll, A. H.; Walter, M. R. Evidence for low sulphate and anoxia in a mid-Proterozoic marine basin. *Nature* **2003**, 423 (6940), 632–635. doi: 10.1038/nature01651
S28. Page, R. W.; Sweet, I. P. Geochronology of basin phases in the western Mt Isa Inlier, and correlation with the McArthur Basin. *Australian Journal of Earth Sciences* **1998**, 45 (2), 219–232. doi: 10.1080/08120099808728383

S29. Large, R. R.; Bull, S. W.; McGoldrick, P. J.; Walters, S. G. Stratiform and Strata-Bound Zn- Pb-Ag Deposits in Proterozoic Sedimentary Basins, Northern Australia. *Economic Geology* **2005**, 100, 931–963.
S30. Brocks, J. J.; Love, G. D.; Summons, R. E.; Knoll, A. H.; Logan, G. A.; Bowden, S. A. Biomarker evidence for green and purple sulphur bacteria in a stratified Palaeoproterozoic sea. *Nature* **2005**, 437 (7060), 866–870. doi: 10.1038/nature04068
S31. Brocks, J. J.; Schaeffer, P. Okenane, a biomarker for purple sulfur bacteria (Chromatiaceae), and other new carotenoid derivatives from the 1640 Ma Barney Creek Formation. *Geochimica et Cosmochimica Acta* **2008**, 72 (5), 1396–1414. doi: 10.1016/j.gca.2007.12.006
S32. Lee, C.; Brocks, J. J. Identification of carotane breakdown products in the 1.64 billion year old Barney Creek Formation, McArthur Basin, northern Australia. *Organic Geochemistry* **2011**, 42 (4), 425–430. doi: 10.1016/j.orggeochem.2011.02.006
S33. Bull, S. W. Sedimentology of the Palaeoproterozoic Barney Creek formation in DDH BMR McArthur 2, southern McArthur basin, northern territory. *Australian Journal of Earth Sciences* **1998**, 45 (1), 21–31. doi: 10.1080/08120099808728364
S34. Jackson, M. J.; Sweet, I. P.; Powell, T. G. Revised sub-division and regional correlation of the McArthur Basin succession based on NABRE's 1995-8 sequence stratigraphic studies. *Australian Geological Survey Organization Record* **2000**, 03.
S35. Jackson, J.; Sweet, I. P.; Powell, T. G. Studies on petroleum geology and geochemistry, mid- dle Proterozoic, McArthur Basin Northern Australia I: Petroleum potential. *The APPEA Journal* **1988**, 28 (1), 283–302. doi: 10.1071/aj87022
S36. Poulton, S. W.; Fralick, P. W.; Canfield, D. E. Spatial variability in oceanic redox structure 1.8 billion years ago. *Nature Geoscience* **2010**, 3 (7), 486–490. doi: 10.1038/ngeo889
S37. Morey, G. Stratigraphic framework of Middle Precambrian rocks in Minnesota. In: Morey, G. Huronian Stratigraphy and Sedimentation, *Geological Association of Canada* **1973**, 12, pp. 211–249.
S38. Addison, W. D.; Brumpton, G. R.; Vallini, D. A.; McNaughton, N. J.; Davis, D. W.; Kissin, S. A.; Fralick, P. W.; Hammond, A. L. Discovery of distal ejecta from the 1850 Ma Sudbury impact event. *Geology* **2005**, 33 (3), 193–196. doi: 10.1130/G21048.1
S39. Needham, R. S.; Stuart-Smith, P. G.; Page, R. W. Tectonic evolution of the Pine Creek Inlier, Northern Territory. *Precambrian Research* **1988**, 40-41, 543–564. doi: 10.1016/0301-9268(88)90084-8
S40. Worden, K.; Carson, C.; Scrimgeour, I.; Lally, J.; Doyle, N. A revised Palaeoproterozoic chronostratigraphy for the Pine Creek Orogen, northern Australia: Evidence from SHRIMP U–Pb zircon geochronology. *Precambrian Research* **2008**, 166 (1-4), 122–144. doi: 10.1016/j.precamres.2007.05.009
S41. Coetzee, L. L. Genetic stratigraphy of the paleoproterozoic Pretoria Group in the Western Transvaal. MSc Thesis **2001**. URL: https://ujcontent.uj.ac.za/vital/access/manager/Repository/uj:14830
S42. Hannah, J. L.; Bekker, A.; Stein, H. J.; Markey, R. J.; Holland, H. D. Primitive Os and 2316 Ma age for marine shale: implications for Paleoproterozoic glacial events and the rise of atmospheric oxygen. *Earth and Planetary Science Letters* **2004**, 225 (1), 43–52. doi: 10.1016/j.epsl.2004.06.013
S43. Rouxel, O. J.; Bekker, A.; Edwards, K. Iron Isotope Constraints on the Archean and Paleopro- terozoic Ocean Redox State. *Science* **2005**, 307 (5712), 1088–1091. doi: 10.1126/science.1105692
S44. Smith, R. E.; Perdrix, J. L.; Parks, T. C. Burial Metamorphism in the Hamersley Basin, Western Australia. *Journal of Petrology* **1982**, 23 (1), 75–102. doi: 10.1093/petrology/23.1.75
*S45. Trendall, A. F.; Nelson, D. R.; Laeter, J. R. D.; Hassler, S. W. Precise zircon U-Pb ages from the Marra Mamba Iron Formation and Wittenoom Formation, Hamersley Group, Western Australia. Australian Journal of Earth Sciences **1998**, 45 (1), 137–142. doi: 10.1080/08120099808728374*
S46. Nelson, D. R.; Trendall, A. F.; Altermann, W. Chronological correlations between the Pilbara and Kaapvaal cratons. *Precambrian Research* **1999**, 97 (3), 165–189. doi: 10.1016/S0301-9268(99)00031-5
S47. Miyano, N. J.; Beukes, T. Phase relations of stilpnomelane, ferri-annite, and riebeckite in very low-grade metamorphosed iron-formations. *South African Journal of Geology* **1984**, 87 (2), 111–124.
S48. Knoll, A. H.; Beukes, N. J. Introduction: Initial investigations of a Neoarchean shelf margin- basin transition (Transvaal Supergroup, South Africa). *Precambrian Research* **2009**, 169 (1-4), 1–14. doi: 10.1016/j.precamres.2008.10.009
S49. Sumner, D. Y.; Bowring, S. A. U-Pb geochronologic constraints on deposition of the Campbell- rand Subgroup, Transvaal Supergroup, South Africa. *Precambrian Research* **1996**, 79 (1), 25–35. doi: 10.1016/0301-9268(95)00086-0

S50. Altermann, W.; Nelson, D. R. Sedimentation rates, basin analysis and regional correlations of three Neoarchaean and Palaeoproterozoic sub-basins of the Kaapvaal craton as inferred from precise U–Pb zircon ages from volcaniclastic sediments. *Sedimentary Geology* **1998**, 120 (1), 225–256. doi: 10.1016/S0037-0738(98)00034-7

S51. Pickard, A. L. SHRIMP U–Pb zircon ages for the Palaeoproterozoic Kuruman Iron Formation, Northern Cape Province, South Africa: evidence for simultaneous BIF deposition on Kaapvaal and Pilbara Cratons. *Precambrian Research* **2003**, 125 (3), 275–315. doi: 10.1016/S0301-9268(03)00113-X

S52. Kendall, B.; Reinhard, C. T.; Lyons, T. W.; Kaufman, A. J.; Poulton, S. W.; Anbar, A. D. Pervasive oxygenation along late Archaean ocean margins. *Nature Geoscience* **2010**, 3 (9), 647–652. doi: 10.1038/ngeo942

S53. Beukes, N. J.; Cairncross, B. A lithostratigraphic-sedimentological reference profile for the late Archaean Mozaan Group, Pongola Sequence; application to sequence stratigraphy and correlation with the Witwatersrand Supergroup. *South African Journal of Geology* **1991**, 94 (1), 44–69.

S54. Elworthy, T.; Eglington, B. M.; Armstrong, R. A.; Moyes, A. B. Rb-Sr isotope constraints on the timing of late to post-Archaean tectonometamorphism affecting the southeastern Kaapvaal Craton. *Journal of African Earth Sciences* **2000**, 30 (3), 641–650. doi: 10.1016/S0899-5362(00)00043-9

S55. Luskin, C.; Wilson, A.; Gold, D.; Hofmann, A. The Pongola Supergroup: Mesoarchaean Deposition Following Kaapvaal Craton Stabilization. In: *The Archaean Geology of the Kaapvaal Craton, Southern Africa.* Kröner, A. and Hofmann, A. (Eds.), Springer, pp. 225-254. doi: 10.1007/978-3-319-78652-0_9

S56. Hicks, N.; Hofmann, A. Stratigraphy and provenance of the auriferous-uraniferous, fluvial to shallow-marine Sinqeni Formation, Mozaan Group, northern Kwazulu-Natal, South Africa. *South African Journal of Geology* **2012**, 115 (3), 327–344. doi: 10.2113/gssajg.115.3.327

S57. Planavsky, N. J.; Asael, D.; Hofmann, A.; Reinhard, C. T.; Lalonde, S. V.; Knudsen, A.; Wang, X.; Ossa Ossa, F.; Pecoits, E.; Smith, A. J. B.; Beukes, N. J.; Bekker, A.; Johnson, T. M.; Konhauser, K. O.; Lyons, T. W.; Rouxel, O. J. Evidence for oxygenic photosynthesis half a billion years before the Great Oxidation Event. *Nature Geoscience* **2014**, 7 (4), 283–286. doi: 10.1038/ngeo2122

S58. Ossa Ossa, F.; Hofmann, A.; Vidal, O.; Kramers, J. D.; Belyanin, G.; Cavalazzi, B. Unusual manganese enrichment in the Mesoarchean Mozaan Group, Pongola Supergroup, South Africa. P*recambrian Research* **2016**, 281, 414–433. doi: 10.1016/j.precamres.2016.06.009

S59. Lowe, D. R. Geologic evolution of the Barberton Greenstone Belt and vicinity. In: Special Paper 329: Geologic Evolution of the Barberton Greenstone Belt, South Africa. Vol. 329. *Geological Society of America* **1999**, pp. 287–312.

S60. Tice, M. M.; Bostick, B. C.; Lowe, D. R. Thermal history of the 3.5–3.2 Ga Onverwacht and Fig Tree Groups, Barberton greenstone belt, South Africa, inferred by Raman microspectroscopy of carbonaceous material. *Geology* **2004**, 32 (1), 37–40. doi: 10.1130/G19915.1

S61. Kröner, A.; Byerly, G. R.; Lowe, D. R. Chronology of early Archaean granite-greenstone evo- lution in the Barberton Mountain Land, South Africa, based on precise dating by single zircon evaporation. *Earth and Planetary Science Letters* **1991**, 103 (1), 41–54. doi: 10.1016/0012-821X(91)90148-B